DEPENDENCE OF Δ_0 AND T_c ON $\alpha^2(\Omega)F(\Omega)$

By

BOŽIDAR MITROVIĆ, B.SC.

A Thesis

Submitted to the School of Graduate Studies

in Partial Fulfilment of the Requirements

for the Degree

Master of Science

McMaster University

December 1979

MASTER OF SCIENCE (1979) McMASTER UNIVERSITY
(Physics) Hamilton, Ontario

TITLE: Dependence of Δ_0 and T_c on $\alpha^2(\Omega)F(\Omega)$

AUTHOR: Božidar Mitrović, B.Sc. (Belgrade University)

SUPERVISOR: Professor J. P. Carbotte

NUMBER OF PAGES: iv,50

ABSTRACT

We have applied the method of N-point Padé approximants to calculate the zero temperature gap edge Δ_0 from the solutions of the Eliashberg equations on the imaginary frequency axis for over thirty isotropic or 'dirty' superconductors. The same method was used in the numerical calculations of the functional derivative $\delta\Delta_0/\delta\alpha^2(\Omega)F(\Omega)$ for several 'dirty' superconductors. Using this functional derivative and the functional derivative of the superconducting critical temperature T_c with respect to the electron-phonon spectral function, $\delta T_c/\delta\alpha^2(\Omega)F(\Omega)$, we have also calculated the functional derivative $\delta(2\Delta_0/k_BT_c)/\delta\alpha^2(\Omega)F(\Omega)$. The universal shape of these functions should prove useful in correlating changes in the zero temperature gap edge Δ_0 and the ratio $2\Delta_0/k_BT_c$ with small changes in the electron-phonon spectral function $\alpha^2(\Omega)F(\Omega)$ with pressure, alloying, increasing disorder, etc.

ACKNOWLEDGMENTS

I would like to thank my supervisor, Professor J. P. Carbotte for his guidance throughout my work. His assistance and encouragement were a great aid in developing this work.

I wish to thank Dr. J. M. Daams for providing her computer programs and help with the programming.

I would like to thank Dr. C. R. Leavens, with whom a part of this project was completed.

I owe many thanks to Dr. F. W. Kus for helpful discussions and aid with the programming.

Mrs. Helen Kennelly, who typed the manuscript, deserves my sincere gratitude.

Finally, I gratefully acknowledge the financial support from McMaster University in the form of a Graduate Assistantship, Dawes Memorial Bursary and Dalley Fellowship, and from National Research Council of Canada in the form of research grants to Dr. Carbotte.

TABLE OF CONTENTS

CHAPTER I

INTRODUCTION

Present day theory of superconductivity[1-4] is quite successful in explaining many experimental phenomena in a quantitative way. The theory is based on the so-called Eliashberg gap equations which relate the parameters of the essential microscopic interactions, to various physical properties of the system. The equations are used both ways: they are either used to extract from experiments quantitative information about the microscopic interactions in various materials (like in tunneling experiments) or to predict various physical properties of superconductors from the knowledge of the basic interaction parameters. From the mathematical point of view these equations are quite complicated and have to be solved numerically on a computer. A purely technical, but of practical importance, problem arises as to how to solve these equations in the most efficient and accurate way. In Chapter II we give a brief discussion of the strong coupling theory of superconductivity emphasizing essential physical aspects of the theory. In Chapter III we apply the method of N-point Padé approximants to the analytic continuation of imaginary axis solution of the Eliashberg equations to the real axis in order to calculate the

ratio $2\Delta_0/k_BT_c$ (a quantity most sensitive to the details of the electron-phonon interaction) for more than thirty superconductors. This technique was recently developed by Vidberg and Serene and we have used it as a supplement to the program written by Dr. J. M. Daams which solves the Eliashberg equations on the imaginary frequency axis.

The concept of functional derivatives, first applied in superconductivity by Bergmann and Reiner, proved to be very useful in investigating how the details of the electron-phonon interaction influence the various physical properties of strong coupling superconductors. In Chapter IV we give the first accurate numerical calculation of the functional derivatives $\delta\alpha_0/\delta\alpha^2(\Omega)F(\Omega)$ and $\delta(2\Delta_0/k_BT_c)/\delta\alpha^2(\Omega)F(\Omega)$ for Ta, Nb, Pb and Nb_3Sn. The universal form of these functional derivatives is revealed. This fact makes them useful in predicting and correlating qualitative changes in the gap edge Δ_0 and the ratio $2\Delta_0/k_BT_c$ to small changes in the electron-phonon spectral function $\alpha^2(\Omega)F(\Omega)$. We also include in Chapter IV one example of such an analysis.

CHAPTER II

ELIASHBERG EQUATIONS

In this chapter we write down the basic equations of the strong coupling theory of superconductivity. The detailed derivation of these, so called, Eliashberg equations falls outside the scope of this thesis and can be found in the literature[1-4]. Instead we will try to point out the main differences between the Bardeen-Cooper-Schrieffer theory of superconductivity (BCS theory) and strong coupling theory.

The physical model of the metal used in BCS theory of superconductivity is the one given by the Landau theory of Fermi liquids. In this theory it is assumed that the low lying excited states of an interacting Fermi gas can be described by the set of long-lived quasi-particles and that these quasi particles have some residual interaction. This residual interaction consists of two parts: one is the screened direct Coulomb interaction which is repulsive and the other is the exchange of virtual phonons which can lead to the attractive interaction between quasi particles provided that their energy (with respect to the Fermi level) is less than the phonon energy. Bardeen, Cooper and Schrieffer have shown that in the case when the total residual interaction is attractive at the Fermi level the Fermi sea becomes unstable against the

formation of the Cooper pairs and that the new superconducting ground state is energetically more favorable than the normal state. The BCS theory of superconductivity was capable of explaining a great many properties of superconductors assuming an instantaneous two-body interaction

$$V_{\underline{k},\underline{k}'} = \begin{cases} -V \text{ , for } \underline{k},\underline{k}' \text{ within the rim of width} \\ \quad 2\hbar\omega_D \text{ centred at the Fermi surface} \\ 0 \text{ , otherwise} \end{cases} \qquad (2.1)$$

where $V > 0$ is essentially an arbitrary constant fitted, say, to the experimental critical temperature and ω_D is the Debye frequency. However, certain deviations from the predictions of the BCS theory have been observed in experiments with particular materials like Pb and Hg, which can be characterized by a high superconducting transition temperature T_c and a low Debye temperature θ_D. Out of many of these deviations we will mention here just two which are relevant to later work.

1) BCS theory predicts that the ratio $2\Delta_0/k_BT_c$ where Δ_0 is the zero temperature gap in the quasi-particle excitation spectrum, k_B - Boltzmann's constant, has the same value 3.53 for all superconductors in the weak coupling limit $N(0)V << 1$, where $N(0)$ is the single-spin density of states at the Fermi level and V is the interaction potential from (2.1). However, experimentally observed values of the ratio

for, say Pb and Hg are 4.52 and 4.60 respectively.

2) For the density of quasi-particle states in a superconductor at zero temperature BCS theory predicts

$$N^{(s)}(\omega) = \begin{cases} N(0) \dfrac{|\omega|}{\sqrt{\omega^2-\Delta_0^2}} , & |\omega| > \Delta_0 \\ 0 , & |\omega| < \Delta_0 \end{cases} \qquad (2.2)$$

It turns out that this density of states can be measured in the single particle tunneling experiments in which one measures the I-V characteristics of a normal metal-oxide-superconductor junction. Experimentally deviations of the order $(\Delta_0/\omega_D)^2$ from the BCS prediction (2.1) have been observed.

One can argue that the BCS ratio $2\Delta_0/k_BT_c = 3.53$ is valid only in the weak coupling limit $N(0)V << 1$ and that the observed deviations can be accounted for within the BCS by abandoning the weak coupling limit. However this is not correct. There are two reasons why BCS theory gives predictions which are not in complete agreement with experimental results. First of all, the attractive interaction between quasi-particles mediated by phonons is retarded in time. This can be understood qualitatively through the following 'hand waving' argument: Suppose that the first electron passes through the middle of a cell of ions and initiates a polarization by attracting the positive ions. Let us

assume that the ions respond by performing simple harmonic motion with frequency equal to the typical phonon frequency ω_D. Then it requires a time $t = \pi/2\omega_D$ for the polarization to develop fully, that is for the ions to reach the maximum distance from their equilibrium positions. The second electron feels the polarized lattice and is attracted toward the place where the first electron used to be. We see that the smaller Debye frequency the longer the retardation that can be expected. Swihart[5] used a variety of nonretarded interactions in calculating the ratio $2\Delta_0/k_B T_c$ and his results were always less than the observed values for Pb and Hg.

Connected to the time dependence of the electron-phonon interaction is the quasi-particle damping. Now, the Landau theory of Fermi liquids, which forms the basis of the BCS theory of superconductivity, is valid provided the damping rate $1/\tau_k$, where τ_k is the life-time of the quasi-particle with energy ε_k, is sufficiently small. More precisely, it is necessary that the quasiparticle level width $\Gamma_k = 1/2\ \tau_k$ is small compared to ε_k

$$\frac{1}{2\tau_k} \equiv \Gamma_k << \varepsilon_k \qquad (2.3)$$

In a metal there are two processes which contribute to the Γ_k. One of them is the particle-hole creation from the electron sea. For sufficiently low temperatures, when only ex-

cited states near the Fermi surface are populated, the Pauli principle restricts the phase space available for the outgoing particles and hole, which results in a small damping rate of the quasi-particles due to this type of process. On the other hand, the contribution to Γ_k arising from the phonon emission satisfies (2.3) only for energies which are very small or very large in comparison with the Debye energy ω_D. For $\varepsilon_k \sim \omega_D$ the ratio Γ_k/ε_k is of the order g^2, the square of the electron phonon coupling constant. It is obvious then that in the case of strong coupling materials like Pb or Hg, where $g^2 \sim 1$, the Landau theory cannot be applied for the temperatures of the order $\theta_D = \omega_D/k_B$ ($\hbar = 1$) or for the processes which involve energies of the order ω_D, regardless of the temperature. The latter is precisely the case in a superconductor where the pairing correlations involve virtually excited states up to ω_D. The theory which deals with this strongly coupled electron-phonon system is known as the strong coupling theory of superconductivity. Before we give the basic microscopic equations of this theory it is useful to point out how the increase of the ratio $2\Delta_0/k_BT_c$ for the strong coupling materials like Pb or Hg can be understood on the basis of quasi-particle damping[6]. The damping decreases the effective pairing interaction strength and therefore the transition temperature T_c and the energy gap Δ_0 at zero temperature are both reduced. But, since

the damping rate is larger at higher temperatures, T_c is reduced more than Δ_0. This results in increasing the ratio $2\Delta_0/k_BT_c$.

To treat a strongly coupled electron-phonon system it is necessary to use the methods of quantum field theory. All physically relevant information about the many-body system is contained in the various Green's functions of the fields in question. For the electron-phonon system one calculates the thermodynamic electron Green's function, or rather the corresponding irreducible self-energy which contains the changes due to interactions. In the case when the anisotropy effects are negligible (so called 'dirty' limit) the self-energy equations for a strong coupling superconductor, known as the Eliashberg gap equations, written on the imaginary frequency axis are

$$\phi(i\omega_n)=\pi k_B T \sum_{n=-\infty}^{+\infty} [\lambda_{n-m}-\mu^*(\omega_c)\theta(\omega_c-|\omega_m|)] \frac{\omega_m}{\sqrt{\omega_m^2+\Delta^2(i\omega_m)}} , \quad (2.4)$$

$$\omega_n Z(i\omega_b) = \omega_n + \pi k_B T \sum_{m=-\infty}^{+\infty} \frac{\omega_m}{\sqrt{\omega_m^2+\Delta^2(i\omega_n)}} . \quad (2.5)$$

The gap function Δ is related to the pairing self-energy ϕ and the renormalization function Z by

$$\Delta(i\omega_n) \equiv \phi(i\omega_n)/Z(i\omega_n) \quad (2.6)$$

where

$$i\omega_n \equiv i\pi k_B T(2n+1) \quad (n = 0,\pm1,\pm2,\cdots) \tag{2.7}$$

are Matsubara frequencies at temperature T. The two quantities which characterize a given material are the electron-phonon spectral function $\alpha^2(\Omega)F(\Omega)$ which describes the phonon-mediated electron-phonon interaction and the Coulomb pseudopotential $\mu^*(\omega_c)$ which describes the direct Coulomb repulsion between the electrons and depends somewhat on the cut-off frequency ω_c used to truncate the summation in (2.4). The electron-phonon spectral function enters the equations through the parameters

$$\lambda_n = \int_0^\infty d\Omega\ \alpha^2(\Omega)F(\Omega)\ \frac{2\Omega}{\Omega^2+\omega_n^2}\ . \tag{2.8}$$

It is defined by[7]

$$\alpha^2(\omega)F(\omega) = \frac{\displaystyle\int_{S_F} \frac{dS_{\underline{p}}}{\hbar|v_{\underline{p}}|} \sum_\lambda \int_{S_F} \frac{dS_{\underline{k}}}{\hbar^2|v_{\underline{k}}|} \frac{\Omega}{(2\pi)^3} \left|\bar{g}_{\underline{k},\underline{p},\lambda}\right|^2 \delta(\omega-\omega_\lambda(\underline{p}-\underline{k}))}{\displaystyle\int_{S_F} \frac{dS_{\underline{p}}}{\hbar|v_{\underline{p}}|}}\ . \tag{2.9}$$

where $\bar{g}_{\underline{k},\underline{p},\lambda}$ is the dressed electron-phonon matrix element, $v_{\underline{k}}$ is the Fermi velocity, $\omega_\lambda(\underline{p}-\underline{k})$ is the phonon energy for reduced momentum $\underline{p}-\underline{k}$ and polarization λ, Ω is the volume and integrations are over the Fermi surface. We note that the

phonon density of states is given by

$$F(\omega) = \frac{1}{N} \sum_{\underline{k}\lambda} \delta(\omega - \omega_\lambda(\underline{k})) \qquad (2.10)$$

where N is the number of atoms in the crystal and the sum over $\underline{k}$ is restricted to the first Brillouin zone. It can be seen that $\alpha^2(\omega)F(\omega)$ describes the phonon density of states weighted by the effectiveness of the phonons of frequency ω for causing transition between any two states on the Fermi surface. By the development of pseudopotential theory and experimental techniques for obtaining information about phonons from inelastic neutron scattering, first principle calculations of the electron-phonon spectral function based on the formula (2.9) have become possible[7]. Also it has been shown[8,9] that $\alpha^2(\omega)F(\omega)$ is related to the phonon life-times due to electron phonon interaction,

$$\alpha^2(\omega)F(\omega) = \frac{\hbar}{2\pi N(0)\omega} \sum_{\underline{q}\lambda} \gamma_{\underline{q}\lambda} \delta(\omega - \omega_\lambda(\underline{q})) \qquad (2.11)$$

where N(0) is the single spin electronic density of states at the Fermi surface and $\gamma_{\underline{q}\lambda}$ is the inverse phonon lifetime. $\gamma_{\underline{q}\lambda}$ is related to the width of the neutron group and can be obtained from the inelastic neutron scattering experiments[9].

The Coulomb repulsion parameter $\mu^*(\omega_c)$ is much more difficult to calculate and the present theory gives only an order of magnitude estimate

$$\mu^*(\omega_c) = \frac{N(0)V_s}{1+N(0)V_s \ln(E_F/\omega_c)} , \qquad (2.12)$$

where E_F is the Fermi energy and within Thomas-Fermi theory for screening

$$N(0)V_s = a^2 \ln \frac{1+a^2}{a^2} , \qquad (2.13)$$

$$a = \left(\frac{k_S}{2k_F}\right)^2 , \qquad (2.14)$$

where k_S is the Thomas-Fermi screening wave vector.

However, single particle tunneling experiments can be used for determining both $\alpha^2(\omega)F(\omega)$ and the μ^*. Before we describe how this comes about it is necessary to give the real axis version of the Eliashberg equations

$$\Delta(T,\omega) = \frac{1}{Z(T,\omega)} \int_0^{\omega_c} d\omega' \{\mathrm{Re}\left[\frac{\Delta(T,\omega')}{\omega'^2-\Delta^2(T,\omega')}\right] \int_0^{\infty} d\Omega \alpha^2(\Omega)F(\Omega)$$

$$\times \left[\left(\frac{1}{e^{\beta\Omega}-1} + \frac{1}{e^{-\beta\Omega'}+1}\right)\left(\frac{1}{\omega'+\omega+\Omega+i0^+} + \frac{1}{\omega'-\omega+\Omega-i0^+}\right) -\right.$$

$$\left. - \left(\frac{1}{e^{\beta\Omega}-1} + \frac{1}{e^{\beta\omega'}+1}\right)\left(\frac{1}{-\omega'+\omega+\Omega+i0^+} + \frac{1}{-\omega'-\omega+\Omega-i0^+}\right)\right]$$

$$-\mu^*(\omega_c)\tanh\frac{\beta\omega'}{2}\} \qquad (2.15)$$

where $\beta = 1/(k_B T)$ and

$$[1-Z(T,\omega)]\omega = \int_0^{+\infty} d\omega' \mathrm{Re}\left[\frac{\omega'}{\sqrt{\omega'^2-\Delta^2(T,\omega')}}\right] \int_0^{+\infty} d\Omega\ \alpha^2(\Omega)F(\Omega)$$

$$\times \left[\left(\frac{1}{e^{\beta\Omega}-1}+\frac{1}{e^{-\beta\omega'}+1}\right)\left(\frac{1}{\omega'+\omega+\Omega+i0^{\mp}}-\frac{1}{\omega'-\omega+\Omega-i0^{\mp}}\right)\right.$$

$$\left.+\left(\frac{1}{e^{\beta\Omega}-1}+\frac{1}{e^{\beta\omega'}+1}\right)\left(\frac{1}{-\omega'+\omega+\Omega+i0^{\mp}}-\frac{1}{-\omega'-\omega+\Omega-i0^{\mp}}\right)\right] \quad (2.16)$$

In the case of $T = 0$ these equations reduce to

$$\Delta(\omega) = \frac{1}{Z(\omega)}\int_0^{\omega_c} d\omega'\ \mathrm{Re}\left[\frac{\Delta(\omega)}{\sqrt{\omega'^2-\Delta'(\omega)}}\right](K_+(\omega,\omega')-\mu^*(\omega_c)) \quad (2.17)$$

$$[1-Z(\omega)]\omega = \int_0^{\infty} d\omega'\ \mathrm{Re}\left[\frac{\omega'}{\sqrt{\omega'^2-\Delta^2(\omega')}}\right]K_-(\omega,\omega') \quad (2.18)$$

with

$$K_{\pm}(\omega,\omega') = \int_0^{+\infty} d\Omega\ \alpha^2(\omega)F(\omega)\left[\frac{1}{\omega'+\omega+\Omega+i0^{\mp}} \pm \frac{1}{\omega'-\omega'+\Omega i0^{\mp}}\right]. \quad (2.19)$$

Now, for the tunneling density of states the strong coupling theory of superconductivity gives

$$N^{(s)}(\omega) = N(0)\mathrm{Re}\left\{\frac{|\omega|}{\sqrt{\omega^2-\Delta^2(\omega)}}\right\}. \quad (2.20)$$

This, together with real axis Eliashberg equations, is used to determine $\alpha^2(\omega)F(\omega)$ and μ^* from tunneling experiments:

a certain guess for $\alpha^2(\omega)F(\omega)$ and μ^* is made and the Eliashberg equations are solved for $\Delta(\omega)$ and $Z(\omega)$. Using this solution one calculates the tunneling density of states and compares it with the one obtained in the experiment. If the agreement is not good $\alpha^2(\omega)F(\omega)$ and μ^* are adjusted and the whole procedure is repeated until full convergence is obtained. We note that the actual value of the Coulomb repulsion parameter μ^* depend somewhat on the choice of the cut-off frequency ω_c (usually taken to be $5\omega_D \sim 10\ \omega_D$). Data on $\alpha^2(\omega)F(\omega)$ have been obtained for many materials from tunneling experiments[10]. Using these together with μ^* as input to the Eliashberg equations one can calculate the thermodynamic and transport properties of superconductors and compare them with experiments.

To end we note that Leavens et al.[11] have shown that the sharp cut-off $\theta(\omega_c - |\omega_m|)$, where $\theta(t) = 1$ for $t > 0$ and $= 0$ for $t < 0$, on the imaginary axis becomes somewhat smeared when analytically continued to the real axis. Therefore, one should not expect $\mu^*(\omega_c)$ to be one and the same number on the real and imaginary axis when the same cut-off frequency ω_c is used in real and imaginary axis version of the Eliashberg equations. In the imaginary axis calculations one usually chooses $\mu^*(\omega_c)$ to fit some observable property of the material.

CHAPTER III

ZERO TEMPERATURE GAP EDGE FROM ANALYTIC CONTINUATION

In order to calculate thermodynamic properties of strong coupling superconductors it is sufficient to know the imaginary axis solutions $\Delta(i\omega_n)$ and $Z(i\omega_n)$ of the Eliashberg gap equations (2.4) and (2.5)[12,13]. However, to calculate the transport properties like tunneling, thermal conductivity etc., one needs the real axis solutions of the self-energy equations (2.15) and (2.16), which also give information about the thermodynamics. In both cases one has to use a computer to solve numerically these nonlinear 'integral' equations. From the numerical point of view, it is much easier and less time consuming to solve the imaginary axis version of the Eliashberg equations. Vidberg and Serene[14] have developed a method of obtaining low temperature real axis solutions by approximate analytic continuation of the imaginary axis solution by means of N-point Padé approximants. The N-point Padé approximant to a complex function $u(z)$ of the complex variable z, whose N values u_i $(i = 1,\ldots,N)$ are given at N complex points z_i $(i = 1,\ldots,N)$ is defined[14-15] as a continued fraction

$$C_n(z) = \frac{a_1}{1+} \frac{a_2(z-z_1)}{1+} \cdots \frac{a_n(z-z_{N-1})}{1}, \qquad (3.1)$$

such that

$$C_N(z_i) = u_i \quad (i = 1,\cdots,N) \ . \tag{3.2}$$

The coefficients a_i are then given by the recursion

$$\left.\begin{aligned} a_i &= g_i(z_i) \\ g_1(z_i) &= u_i \end{aligned}\right\} \quad (i=1,\cdots,N) \ , \tag{3.3}$$

$$g_p(z) = \frac{g_{p-1}(z_{p-1}) - g_{p-1}(z)}{(z-z_{p-1})\,g_{p-1}(z)} \quad (p \geq 2) \ . \tag{3.4}$$

It can be shown that

$$C_N(z) = \frac{A_N(z)}{B_N(z)} \tag{3.5}$$

where A_N and B_N are polynomials given by the recursion

$$\begin{aligned} A_{n+1}(z) &= A_n(z) + (z-z_n)\,a_{n+1}A_{n-1}(z) \\ B_{n+1}(z) &= B_n(z) + (z-z_n)\,a_{n+1}B_{n-1}(z) \end{aligned} \qquad (n = 1,2,\cdots N-1) \tag{3.6}$$

and

$$A_0 = 0 \ , \quad A_1 = a_1 \ , \quad B_0 = B_1 = 1 \ . \tag{3.7}$$

Vidberg and Serene[14] have tested this method on several general cases and applied it to the problem of obtaining the real axis solutions $\Delta(\omega)$ and $Z(\omega)$ from the imaginary solutions $\Delta(i\omega_n)$ and $Z(i\omega_n)$ at the Matsubara frequencies.

The main conclusions of their analysis are:

a) In order to get a good approximation to a function structured in the interval $[o,\bar{\omega}]$ on the real axis one should use a sufficient number of input points from the interval $[o,i\omega']$ on the imaginary axis where $i\omega'$ belongs to the range of imaginary axis where the function attains its asymptotic form (usually $i\omega'$ is several times $i\bar{\omega}$).

b) The number of digits in the known values of the function u_i $(i = 1,\ldots,N)$ is crucial for obtaining a good analytic continuation.

c) Overall agreement between the $\Delta(\omega)$ and $Z(\omega)$ obtained by means of N-point Padé approximant and those tabulated by Rowell, McMillan and Dynes[10] is good, being excellent in the low frequency range (from zero up to several millielectron volts).

In their calculations Vidberg and Serene have fitted the Coulomb repulsion parameter to the experimentally observed gap edge Δ_0 at zero temperature, which is, within strong coupling theory, given by the condition

$$\text{Re } \Delta(\omega=\Delta_0) = \Delta_0 \,. \tag{3.8}$$

We have applied the method of N-point Padé approximants to calculate the ratio $2\Delta_0/k_BT_c$ from the Eliashberg theory for many superconductors (see Table 1). In our calculations we have taken a different approach in determining the $\mu^*(\omega_c)$. Namely, we have fitted μ^* to the experimental transition temperature T_c since this quantity can be measured

with better accuracy than the zero temperature gap edge Δ_0. Within the imaginary frequency axis formulation the Eliashberg theory, the critical temperature T_0 is determined as the maximum temperature T at which the linearized gap equations, obtained from (2.4) and (2.5) by setting quadratic terms in the gap equal to zero

$$\phi(i\omega_n) = \pi k_B T \sum_{m=-\infty}^{+\infty} [\lambda_{mn} - \mu^*(\omega_c)\theta(\omega_c - |\omega_m|)] \frac{\Delta(i\omega_m)}{|\omega_m|} \qquad (3.9)$$

$$\omega_n z(i\omega_n) = \omega_n + \pi k_B T \sum_{m=-\infty}^{+\infty} \lambda_{n-m} \mathrm{sgn}(\omega_m) , \qquad (3.10)$$

have a non trivial solution ϕ (that is Δ). For fixed cut-off frequency ω_c we have fitted the $\mu^*(\omega_c)$ to the experimental transition temperature T_c and then used the same cut-off and Coulomb repulsion parameter to solve the Eliashberg equations (2.4) and (2.5) at some low temperature. Then we have applied the Padé scheme and determined Δ_0 from the condition (3.8). Since the Padé scheme is supposed to work well in low frequency range (see c)) one can hope that this method will give a good value for the Δ_0. Furthermore, in view of a), it is not necessary to take too large a cut-off ω_c for the purposes of determining the gap edge at zero temperature. In most cases we have taken ω_c to be three times the maximum phonon frequency ω_M of the given material (see Table 1). The temperature T at which the Eliashberg equations

(2.4) and (2.5) were solved was usually 0.4°K. The variation of $\Delta_0(T)$ - the gap edge at temperature T with T is negligible at very lowtemperatures and one can neglect the difference between $\Delta_0(T=0)$ and $\Delta_0(T)$ for $T << T_c$.

There were several reasons for performing this calculation. First of all we wanted to check this method of obtaining Δ_0, in particular our choice of $\mu^*(\omega_c)$. If this method works well in the case of Pb and Hg, where it is already known that the strong coupling theory of superconductivity works perfectly and single particle tunneling experiments can be done without any difficulty, the validity of the method is justified. Then one can proceed and calculate the ratio $2\Delta_0/k_BT_c$ for other superconductors, since this quantity is most sensitive to the details of the electron-phonon interaction, as we have mentioned in the previous chapter. If the agreement between calculated and experimental ratio $2\Delta_0/k_BT_c$ is not good one can suspect:

i) The quality of tunneling experiment from which the electron-phonon spectral function $\alpha^2(\Omega)F(\Omega)$ is extracted and used in our calculation. In this respect one should be very careful with transition elements since, in this case, it is extremely difficult to make good tunneling junctions by the common method of thermal oxidation. Not very long ago some people were proposing a breakdown of Eliashberg theory in the case of Nb where tunneling results gave surprising results (a negative value

of μ^*, for example). It turned out that the tunneling junctures were bad and the common McMillan-Rowell inversion procedure was giving spurious results on $\alpha^2(\Omega)F(\Omega)$ and μ^*.

ii) The experimental values of T_c and/or Δ_0 since in our procedure we fitted $\mu^*(\omega_c)$ to T_c. It is preferable to use the value of T_c obtained on the sample which is used in tunneling experiments since various properties can vary from sample to sample of one and the same material. Furthermore, even if Δ_0 and T_c are measured on one and the same specimen they can sample different regions of the specimen. Δ_0 gives global information about the surface layers of the superconducting part of the junction while inductively measured T_c corresponds to the region of the highest transition temperature if the sample is inhomogeneous.

iii) Finally one can question the validity of the standard form of Eliashberg equations, in particular the treatment of the electronic density of states which is usually assumed to be constant in the energy interval $2\omega_M$ ($\hbar=1$) around the Fermi level. In the case of A-15 materials the possibility of a rapidly varying electronic density of states in this energy interval is quite realistic.

In Table 1 we give the results of our calculations. In this table A is the area under $\alpha^2(\Omega)F(\Omega)$

$$A = \int_0^{+\infty} d\Omega\ \alpha^2(\omega)F(\omega)\ , \qquad (3.11)$$

λ is the mass enhancement parameter due to the electron-phonon interaction

$$\lambda = 2 \int_0^{+\infty} d\Omega \, \frac{\alpha^2(\Omega)F(\Omega)}{\Omega} \tag{3.12}$$

and $\bar{E}$ is proportional to average phonon energy

$$\bar{E} = \int_0^{+\infty} d\Omega \; \Omega \; \alpha^2(\Omega)F(\Omega) \; . \tag{3.13}$$

μ^*_{tun} is the value of Coulomb repulsion parameter obtained by inversion of the tunneling data and μ^*_{fitted} is the value fitted to the experimental transition temperature T_c with appropriate cut-off frequency ω_c. Δ_0^{exp} is the experimental value of the zero-temperature gap edge and Δ_0^{calc} is the corresponding calculated quantity. We also give $(\Delta_0^{calc}-\Delta_0^{exp})/\Delta_0^{exp}\times 100\%$ and the calculated value $2\Delta_0^{calc}/k_BT_c$. Since we have used experimental values of the critical temperature the relative error in $2\Delta_0^{calc}/k_BT_c$ for the experimental value is the same as the one in Δ_0^{calc}. We note that in the case of Pb and Hg the agreement between the calculated and experimental values of Δ_0 is perfect. Also in the case of Al (here we have used the spectrum $\alpha^2(\Omega)F(\Omega)$ calculated by Leung et al.) the calculated ratio is very close to the BCS result 3.53. Aluminium is a very weak coupling material for which the retardation and damping effects are not important and which can be well described within the BCS theory. We

Table 1

System	ω_M(meV)	A(meV)	λ	$\bar{E}$(meV^2)	ω_c/ω_M	μ^*_{tunn}	μ^*_{fitted}	T_c(°K)	Δ_0^{exp} (meV)	Δ_0^{calc} (meV)	$(\Delta_0^{calc}-\Delta_0^{exp})/\Delta_0^{exp}$ × 100%	$(2\Delta_0/k_BT_c)_{calc}$
Al^{26}	41.4	5.94	0.432	179.51	3	-	0.147216	1.8	-	0.18	-	3.54
Sn^{10}	18.4	3.42	0.716	39.36	3	0.11	0.114317	3.75	0.606	0.599	-1.1	3.71
Nb_3Sn^{16}	28.7	10.65	1.68	168.29	6	0.15	0.1575	18.	3.1	3.53	+13.9	4.55
Nb^{19}	29.	6.31	0.97	102.26	3	0.11	0.1157977	9.2	1.46	1.57	+7.5	3.96
Nb^{22}	28.87765	8.87	1.12	159.04	3	-	0.2734965	9.2	-	1.53	-	3.86
Nb^{21}	28.29	7.25	1.01	120.74	6	0.16	0.1854215	9.22	1.51	1.54	+2	3.88
$Nb_{.75}Zr^{25}_{.25}$	26.	7.425	1.31	107.85	6	0.10 ± 0.02	0.1807988	10.8	1.9	1.93	+1.6	4.15
Ta^{10}	20.9	4.16	0.69	56.9	3	0.11	0.116881	4.48	0.72	0.71	-1.4	3.68
In^{10}	15.8	2.74	0.805	23.76	3	0.125	0.113023	3.40	0.541	0.556	+2.8	3.80
$In_{.9}Tl_{.1}{}^{10}$	16.2	2.74	0.85	23.08	3	0.12	0.127084	3.28	0.530	0.540	+1.9	3.82
$In_{.73}Tl_{.27}{}^{10}$	14.6	2.69	0.934	20.61	3	0.13	0.135756	3.36	0.57	0.564	-1.0	3.90
$In_{.67}Tl_{.33}{}^{10}$	15.2	2.65	0.90	20.68	3	0.13	0.1314141	3.26	0.54	0.543	+0.6	3.87
$In_{.57}Tl_{.43}{}^{10}$	14.4	2.34	0.85	17.15	3	0.14	0.1386705	2.6	0.42	0.426	+1.4	3.80
$In_{.50}Tl_{.50}{}^{10}$	14.8	2.28	0.83	16.40	3	0.13	0.1377337	2.52	0.41	0.41	0.0	3.78
$In_{.27}Tl_{.73}{}^{10}$	13.6	2.48	1.09	16.02	3	0.11	0.116384	3.64	0.64	0.64	0.0	4.08
$In_{.17}Tl_{.83}{}^{10}$	13.2	2.29	0.98	14.44	3	0.12	0.11878	3.19	0.535	0.545	+1.9	3.96
$In_{.07}Tl_{.93}{}^{10}$	11.8	2.16	0.89	13.15	3	0.13	0.1310601	2.77	0.45	0.46	+2.2	3.85

(continued next page)

Table 1 (continued)

System	ω_M(meV)	A(meV)	λ	$\bar{E}$(meV^2)	ω_c/ω_M	μ^*_{tunn}	μ^*_{fitted}	T_c(°K)	Δ_0^{exp} (meV)	Δ_0^{calc} (meV)	$(\Delta_0^{calc}-\Delta_0^{exp})/\Delta_0^{exp}$ × 100%	$(2\Delta_0/k_BT_c)_{calc}$
Tl[10]	10.9	2.0	0.795	12.16	3	0.135	0.1281217	2.36	0.366	0.382	+4.	3.76
$Pb_{.4}Tl_{.6}$[10]	11.	2.74	1.15	16.13	3	0.113	0.1149488	4.60	0.805	0.822	+2.1	4.15
$Pb_{.6}Tl_{.4}$[10]	10.9	3.35	1.38	19.60	3	0.126	0.1261557	5.90	1.08	1.11	+2.8	4.37
$Pb_{.8}Tl_{.2}$[10]	10.9	3.71	1.53	21.32	3	0.122	0.1239405	6.80	1.28	1.33	+3.9	4.54
Pb[10]	11.	4.03	1.55	23.93	3	0.131	0.1445888	7.19	1.40	1.40	0.0	4.52
$Pb_{.9}Bi_{.10}$[10]	9.9	3.98	1.66	22.38	3	0.095	0.1120409	7.65	1.54	1.55	+0.6	4.70
$Pb_{.8}Bi_{.2}$	10.9	4.19	1.88	22.42	3	0.111	0.1126537	7.95	1.61	1.67	+3.7	4.88
$Pb_{.7}Bi_{.3}$[10]	10.4	4.46	2.	23.54	3	0.11	0.1153717	8.45	1.77	1.82	+2.8	5.00
$Pb_{.65}Bi_{.35}$[10]	10.1	4.6	2.13	24.09	3	0.111	0.0995533	8.95	1.84	1.98	+7.6	5.13
$Pb_{.60}Tl_{.20}Bi_{20}$[10]	10.2	4.14	1.82	22.33	3	0.137	0.1537982	7.26	1.50	1.49	-0.7	4.76
$Tl_{.90}Bi_{.10}$[10]	10.5	1.86	0.78	10.97	3	0.119	0.1113920	2.3	0.354	0.374	+5.6	3.77
Hg[10]	14.3	2.645	1.62	14.33	3	0.11	0.119664	4.19	0.83	0.83	0.0	4.60
Amorphous Bi[30]	14.	3.53	2.46	20.06	3	0.105	0.0917228	6.11	1.21	1.30	+7.4	4.94
Amorphous $Pb_{.50}Bi_{.50}$[31]	13.1	4.30	3.00	22.1	3	0.14	0.1337717	6.99	1.51	1.57	+4.	5.21
Amorphous $Pb_{.75}Bi_{.25}$[31]	12.7	4.20	2.76	21.78	3	0.14	0.1339791	6.91	1.48	1.53	+3.4	5.14
Amorphous Ga[31]	27.	6.15	2.25	69.30	3	0.17	0.1631958	8.56	1.68	1.74	+3.6	4.72

see that our procedure gives the correct weak coupling limit of the Eliashberg theory.

Since the experimental results for the gap edge are accurate to at best 1% we can conclude that, except in a few cases, the agreement between the calculated value of the gap edge Δ_0 and the corresponding experimental value is quite good.

The few exceptions deserve special attention. The worst agreement is in the case of Nb_3Sn. For this material we have used the electron phonon spectral function $\alpha^2(\Omega)F(\Omega)$ obtained by Shen[16] from tunneling experiments. Recently, Moore, Zubeck, Rowell and Beasly[17] have performed tunneling experiments in a series of A-15 materials. They have used an improved technique for forming tunneling junctions with these difficult materials. In their experiments on Nb_3Sn the measured values of the zero temperature gap edge Δ_0 are between 3.2 meV and 3.4 meV, that is larger than Shen's value of 3.1 meV and close to our calculated value of 3.53 meV. However there are still some difficulties with the inversion procedure[18] (for example a negative value of μ^*) and it may well be that the standard Eliashberg theory which serves as the basis of present inversion techniques is inappropriate for these materials.

The second example of poor agreement is the case of Nb where we have used the $\alpha^2(\omega)F(\omega)$ obtained by Rowell et al.

from tunneling experiments. The basic characteristics of this spectrum are ω_H = 29 meV, A = 6.31 meV, λ = 0.97 and $\bar{E}$ = 102.26 meV^2. The tunneling junction was made by thermal oxidation of Nb. It turns out[20] that in this way one obtains a thin layer of normal material between the superconducting Nb and the oxide. So the actual structure of the tunneling junction is not any more superconductor-oxide-normal metal (SON) but superconductor-normal metal-oxide-normal metal (SNON). The SN part of the junction acts effectively as a proximity sandwich and alters the I-V characteristics from what one would obtain in the case of a standard SON junction. In principle, it is possible[20] to obtain $\alpha^2(\Omega)F(\Omega)$ from the tunneling density of states in this more complicated situation if one knows the geometry of the proximity sandwich. But in the case of a tunneling junction with a thermally grown oxide on Nb there is no information whatsoever on the thickness of the normal phase layer. Wolf and Arnold[20] were the first to understand this difficulty with Nb and have also found a way around it[21]. The solution was to form a junction of the SNON type but with a N layer (between S and O) which can be thermally oxidized without any problem and with known dimensions. In this way they were able to account for the presence of the proximity sandwich in a quantitative way and extract the $\alpha^2(\Omega)F(\Omega)$ and μ^* for Nb from the tunneling characteristics. We have also calculated the

ratio $2\Delta_0/k_BT_c$ for this spectrum (ω_H = 28.29 meV, A = 7.25 meV, λ = 1.01, $\bar{E}$ = 120.74 meV). As can be seen from Table 1, the agreement between Δ_0^{calc} and Δ_0^{exp} is very good, the error being 2%.

For niobium we have also used the third spectrum obtained by Butler et al.[22] from the analysis of the widths of the neutron groups and their relation to the phonon lifetime due to the electron-phonon interaction (see Chapter II). The basic characteristics of this spectrum are ω_M = 28.87765 meV, A = 8.87 meV, λ = 1.12, $\bar{E}$ = 159.04 meV^2. The calculated value of the gap edge (1.53 meV) is quite close to the one obtained from the previous spectrum (1.54 meV). Therefore, we can say that the Eliashberg theory works well for the transition element Nb and that all the peculiarities of the previously obtained data from the tunneling (like negative μ^*, small value of λ[23]) were the result of bad tunneling junctions. We conclude this discussion of Nb by noting that recently it was proposed by Rietschel and Winter[24] that for transition elements Eliashberg equations should be modified to include 'paramagnons', that is spin fluctuations, which oppose superconductivity. However, the presence of paramagnons can be simulated within standard Eliashberg theory by increasing the Coulomb repulsion parameter μ^*.

At present we do not have an unambiguous explanation for the large discrepancies between calculated and measured

values of the gap edge Δ_0 for the alloy $Pb_{.65}Bi_{.35}$ and amorphous Bi. The most probable answer is that the measured values of the gap edge Δ_0 at zero temperature and/or transition temperature T_c are not accurate for these two materials.

We can conclude this section by saying that the method of N-point Padé approximants for obtaining the zero temperature gap edge from imaginary axis solutions is quite reliable. Second, in most of the cases investigated here standard Eliashberg theory predicts well the observed values of the ratio $2\Delta_0/k_BT_c$.

CHAPTER IV

THE FUNCTIONAL DERIVATIVES $\delta\Delta_0/\delta\alpha^2(\Omega)F(\Omega)$ AND $\delta(2\Delta_0/k_BT_c)/\delta\alpha^2(\Omega)F(\Omega)$

The material properties of a strong coupling superconductor are contained in the electron-phonon spectral function $\alpha^2(\Omega)F(\Omega)$ and Coulomb repulsion parameter μ^*. One can use these quantities to calculate the transition temperature, critical field, zero temperature gap edge Δ_0 and other integral properties of a superconductor, by solving the Eliashberg gap equations. When we say that T_c, Δ_0, etc. are integral properties of a superconductor we mean that these quantities are functionals of $\alpha^2(\omega)F(\omega)$ and μ^*. Several years ago Bergmann and Reiner[12] applied the notion of functional derivative to investigate the effectiveness of various phonon frequencies in determining the critical tempature T_c and other thermodynamic properties of superconductors. The functional derivative they have used is defined by

$$\frac{\delta T_c}{\delta\alpha^2(\Omega)F(\Omega)} = \lim_{\varepsilon\to 0} \frac{T_c[\alpha^2(\omega)F(\omega)+\varepsilon\delta(\omega-\Omega)]-T_c[\alpha^2(\omega)F(\omega)]}{\varepsilon} \qquad (4.1)$$

where $\delta(\omega-\Omega)$ is Dirac's delta-function. The physical significance of this functional derivative is evident from the relation

$$\Delta T_c = \int_0^{+\infty} d\Omega \, \frac{\delta T_c}{\delta \alpha^2(\Omega) F(\Omega)} \, \delta \alpha^2(\Omega) F(\Omega) \qquad (4.2)$$

where ΔT_c is the change in critical temperature due to a small change $\delta \alpha^2(\Omega) F(\Omega)$ in electron-phonon spectral function. Since they were concerned with thermodynamic properties of superconductors they were able to work within the imaginary axis version of the Eliashberg equations. Their numerical calculations of $\delta T_c / \delta \alpha^2(\Omega) F(\Omega)$ for many superconductors indicated that this derivative has a universal shape: it increases linearly from zero at $\Omega = 0$ to a maximum at $\Omega \approx 8 k_B T_c$ and then decreases slowly to zero as $\Omega \to \infty$. One can understand why this functional derivative peaks at $\Omega \approx 8 k_B T_c$ through the following 'hand-waving' argument due to Carbotte and Leavens, which is similar to the one used in Chapter II to explain the retarded nature of the electron-phonon interaction: First, an electron passing through the middle of a cell of ions attracts the ions and induces simple harmonic motion with average frequency Ω. Then a second electron will derive maximum benefit from the polarization if it arrives at time $t = \pi/2\Omega$ after the polarization has been initiated at the point where the first electron used to be. On the other hand this time is determined by the initial separation of electrons which is equal to the coherence distance ξ_0 (a measure of the spatial extent of the Cooper pair) and by the Fermi velocity v_F at which

electrons move: $v_F t = \xi_0$. Therefore $\Omega = \frac{\pi}{2}\frac{v_F}{\xi_0}$. Substituting the expression $\xi_0 = (7\zeta(3)/4)^{1/2} v_F/2\pi k_B T_c$ for the coherence length describing the spatial range of fluctuations gives $\Omega = \frac{\pi^2}{1.45} k_B T_c \approx 7 k_B T_c$.

We have used the method of N-point Padé approximant to obtain the zero temperature gap edge Δ_0 from the imaginary axis solution of Eliashberg equations and to calculate the functional derivatives

$$\frac{\delta \Delta_0}{\delta \alpha^2(\Omega) F(\Omega)} \tag{4.3}$$

and

$$\frac{\delta}{\delta \alpha^2(\Omega) F(\Omega)} \left(\frac{2\Delta_0}{k_B T_c}\right) = \frac{2\Delta_0}{k_B T_c} \left[\frac{1}{\Delta_0} \frac{\delta \Delta_0}{\delta \alpha^2(\Omega) F(\Omega)} - \frac{1}{T_c} \frac{\delta T_c}{\delta \alpha^2(\Omega) F(\Omega)}\right] \tag{4.4}$$

for Ta[10], Nb[9], Pb[10] and Nb_3Sn[16] and thereby resolve the question of how effective are various phonon frequencies in contributing to Δ_0 or to the ratio $2\Delta_0/k_B T_c$.

Before we describe the method of calculating functional derivatives (4.3) and (4.4), and the obtained results it is interesting to see what we can expect on the basis of a 'hand-waving' argument. Expressing the coherence length ξ_0 in terms of the zero-temperature gap Δ_0, $\xi_0 = v_F/\pi\Delta_0$ we obtain for the optimum phonon frequency in enhancing the gap $\Omega = \pi^2\Delta_0/2 \approx 5\Delta_0$; however if in the previous result $\Omega = (\pi^2/1.45) k_B T_c$ we substitute $k_B T_c$ given by $2\Delta_0/k_B T_c = 4$ we get

for the optimum phonon frequency $\Omega \approx \frac{\pi^2}{3}\Delta_0 \approx 3\Delta_0$. Therefore, on the basis of this simple argument we can expect that the most effective frequencies in contributing to the gap parameter Δ_0 are of the order of several Δ_0.

We calculate the functional derivative $\delta\Delta_0/\delta\alpha^2(\Omega)F(\Omega)$ on the basis of the defining formula

$$\frac{\delta\Delta_0}{\delta\alpha^2(\Omega)F(\Omega)} = \lim_{\varepsilon\to 0} \frac{\Delta_0[\alpha^2(\Omega)F(\Omega)+\varepsilon\delta(\Omega-\Omega')]-\Delta_0[\alpha^2(\Omega)F(\Omega)]}{\varepsilon} \quad (4.5)$$

by augmenting $\alpha^2(\Omega)F(\Omega)$ by a histogram centered at Ω' of sufficiently small height and width and then computing the resulting change in the gap edge. This method of calculating the functional derivative was checked with the case of $\delta T_c/\delta\alpha^2(\omega)F(\omega)$ for Ta which can be obtained within the imaginary axis formulation with a better numerical precision[12-13]. The agreement was good to within a few percent.

For the special case $\Omega = 0$ the functional derivative $\delta\Delta_0/\delta\alpha^2(\Omega)F(\Omega)$ can be calculated analytically. If we replace $\phi(i\omega_n)$ on the lef-hand side of (2.4) by $\Delta(i\omega_n)Z(i\omega_n)$ and then use (2.5) to eliminate $Z(i\omega_n)$ we obtain

$$\Delta(i\omega_n) = \pi k_B T \Big\{ \sum_{m=-\infty}^{+\infty} \lambda_{n-m} \Big[\frac{\Delta(i\omega_m)-(\omega_m/\omega_n)\Delta(i\omega_n)}{\sqrt{\omega_m^2+\Delta^2(i\omega_m)}}\Big]$$

$$- \mu^*(\omega_c) \sum_{m=-\infty}^{+\infty} \Big[\frac{\theta(\omega_c)-|\omega_m|)\Delta(i\omega_m)}{\sqrt{\omega_m^2+\Delta^2(i\omega_m)}}\Big] \Big\} .$$

*For m = n

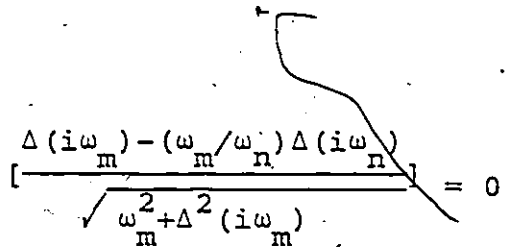

$$\left[\frac{\Delta(i\omega_m)-(\omega_m/\omega_n)\Delta(i\omega_n)}{\sqrt{\omega_m^2+\Delta^2(i\omega_m)}}\right] = 0$$

so that $\Delta(i\omega_n)$ does not depend on $\lambda_0 = \lambda$. Furthermore for $m \neq n$

$$\lambda_{m-n}(\alpha^2(\Omega)F(\Omega)+\varepsilon\delta(\Omega)) = 2\int_0^{+\infty} d\Omega\ \frac{[\alpha^2(\Omega)F(\Omega)+\varepsilon\delta(\Omega)]}{\Omega^2+(\omega_m-\omega_n)^2} =$$

$$= 2\int_0^{+\infty} d\Omega\ \frac{\Omega\alpha^2(\Omega)F(\Omega)}{\Omega^2+(\omega_m-\omega_n)^2} = \lambda_{m-n}(\alpha^2(\Omega)F(\Omega)$$

so that augmenting $\alpha^2(\Omega)F(\Omega)$ by $\varepsilon\delta(\Omega)$ has no effect on λ_{n-m} for $n \neq m$. Since $\Delta(i\omega_n)$, and therefore $\Delta(\omega)$, depends only on λ_{m-n} with $m \neq n$, the solution doesn't change when $\alpha^2(\Omega)F(\Omega)$ is replaced by $\alpha^2(\Omega)F(\Omega)+\varepsilon\delta(\Omega)$ for any ε, and we have

$$\left.\frac{\delta\Delta_0}{\delta\alpha^2(\Omega)F(\Omega)}\right|_{\Omega=0} = 0\ . \qquad (4.6)$$

In figures 1-4 we plot $\Delta_0^{-1}\delta\Delta_0/\delta\alpha^2(\Omega)F(\Omega)$ and $T_c^{-1}\delta T_c/\delta\alpha^2(\Omega)F(\Omega)$ for the superconductors Ta, Nb, Pb and Nb_3Sn, respectively. We note that the functional derivative $\delta T_c/\delta\alpha^2(\Omega)F(\Omega)$ was calculated with the program written by Dr. J. M. Daams. There are two common features of the four plots. First, $\delta T_c/\delta\alpha^2(\Omega)F(\Omega)$ peaks at a frequency $\Omega^*(T_c)$ which is within $\sim$ 5% of twice the peak frequency $\Omega^*(\Delta_0)$ of

FIG. 1

$\Delta_0^{-1}\delta\Delta_0/\delta\alpha^2(\Omega)F(\Omega)$ (———) and $T_c^{-1}\delta T_c/\delta\alpha^2(\Omega)F(\Omega)$ (·····) for Ta.

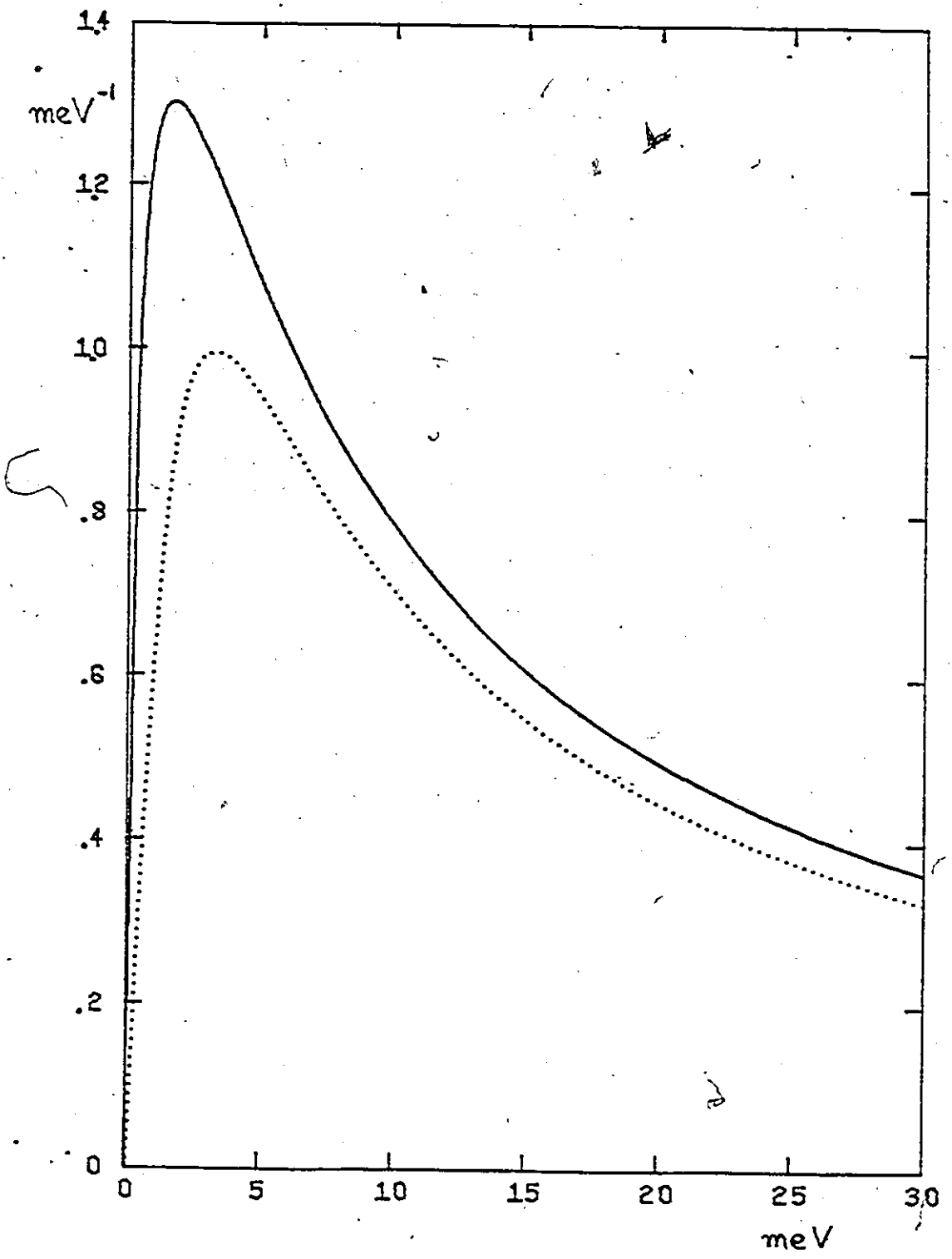
1.4
meV⁻¹
1.2
1.0
.8
.6
.4
.2
0
0
5
10
15
20
25
30
meV

FIG. 2

$\Delta_0^{-1}\delta\Delta_0/\delta\alpha^2(\Omega)F(\Omega)$ (———) and $T_c^{-1}\,T_c/\delta\alpha^2(\Omega)F(\Omega)$ (·····) for Nb.

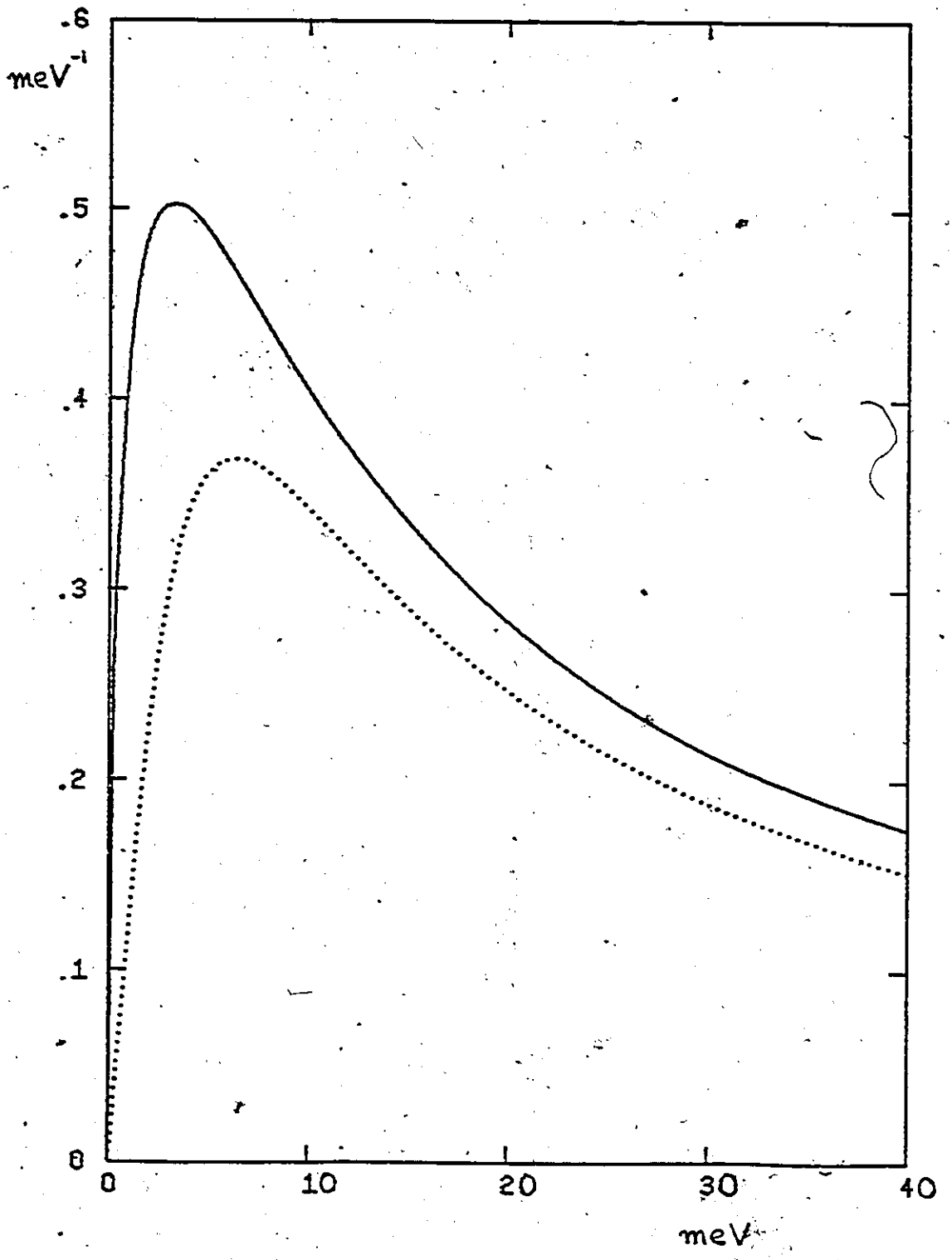
.6
meV⁻¹
.5
.4
.3
.2
.1
0
0
10
20
30
40
meV

FIG. 3

$\Delta_0^{-1}\delta\Delta_0/\delta\alpha^2(\Omega)F(\Omega)$ (———). and $T_c^{-1}\delta T_c/\delta\alpha^2(\Omega)F(\Omega)$ (·····) for Pb.

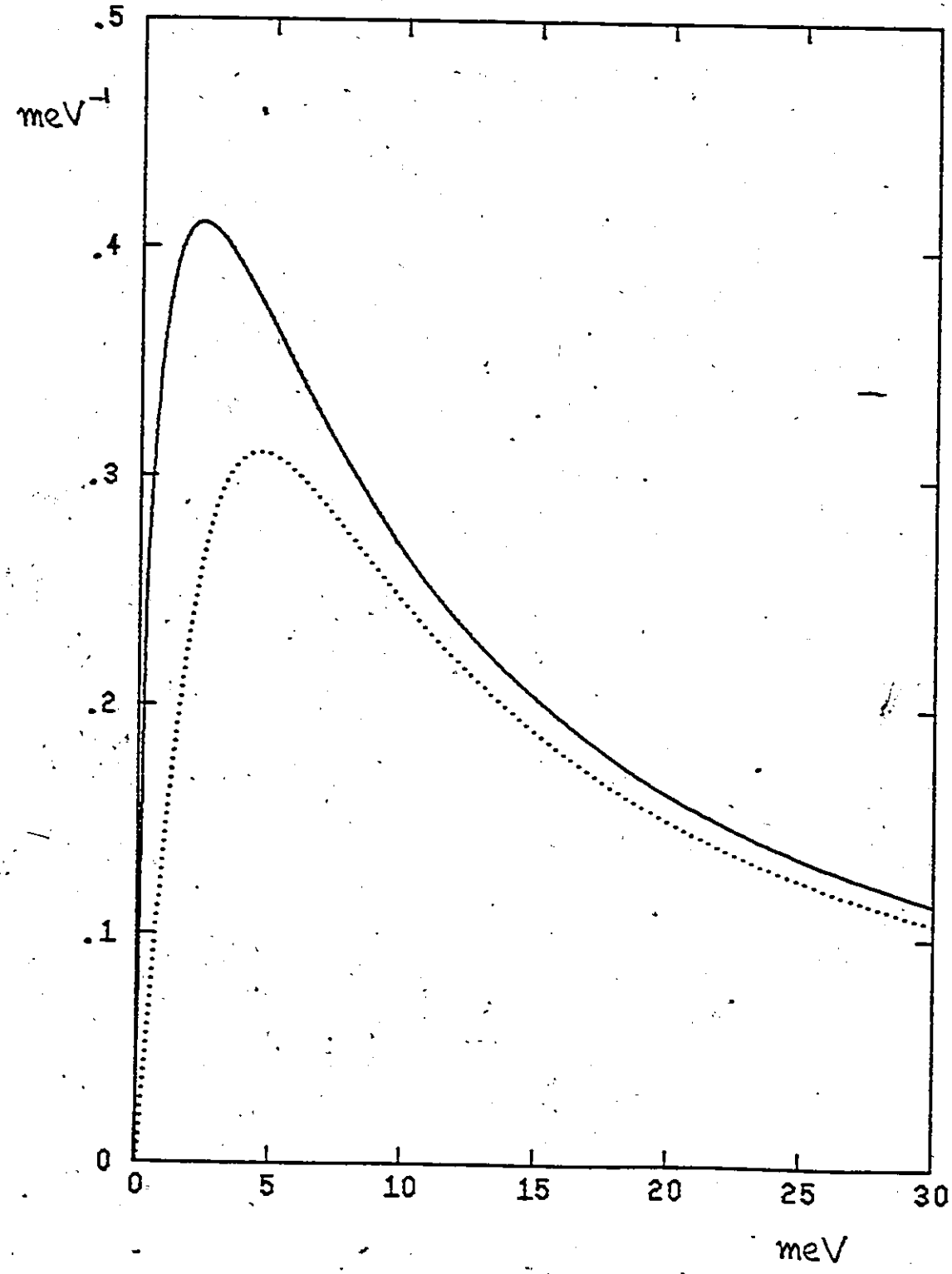
.5
meV⁻¹
.4
.3
.2
.1
0
0
5
10
15
20
25
30
meV

FIG. 4

$\Delta_0^{-1}\delta\Delta_0/\delta\alpha^2(\Omega)F(\Omega)$ (———) and $T_c^{-1}\delta T_c/\delta\alpha^2(\Omega)F(\Omega)$ (·····) for Nb_3Sn.

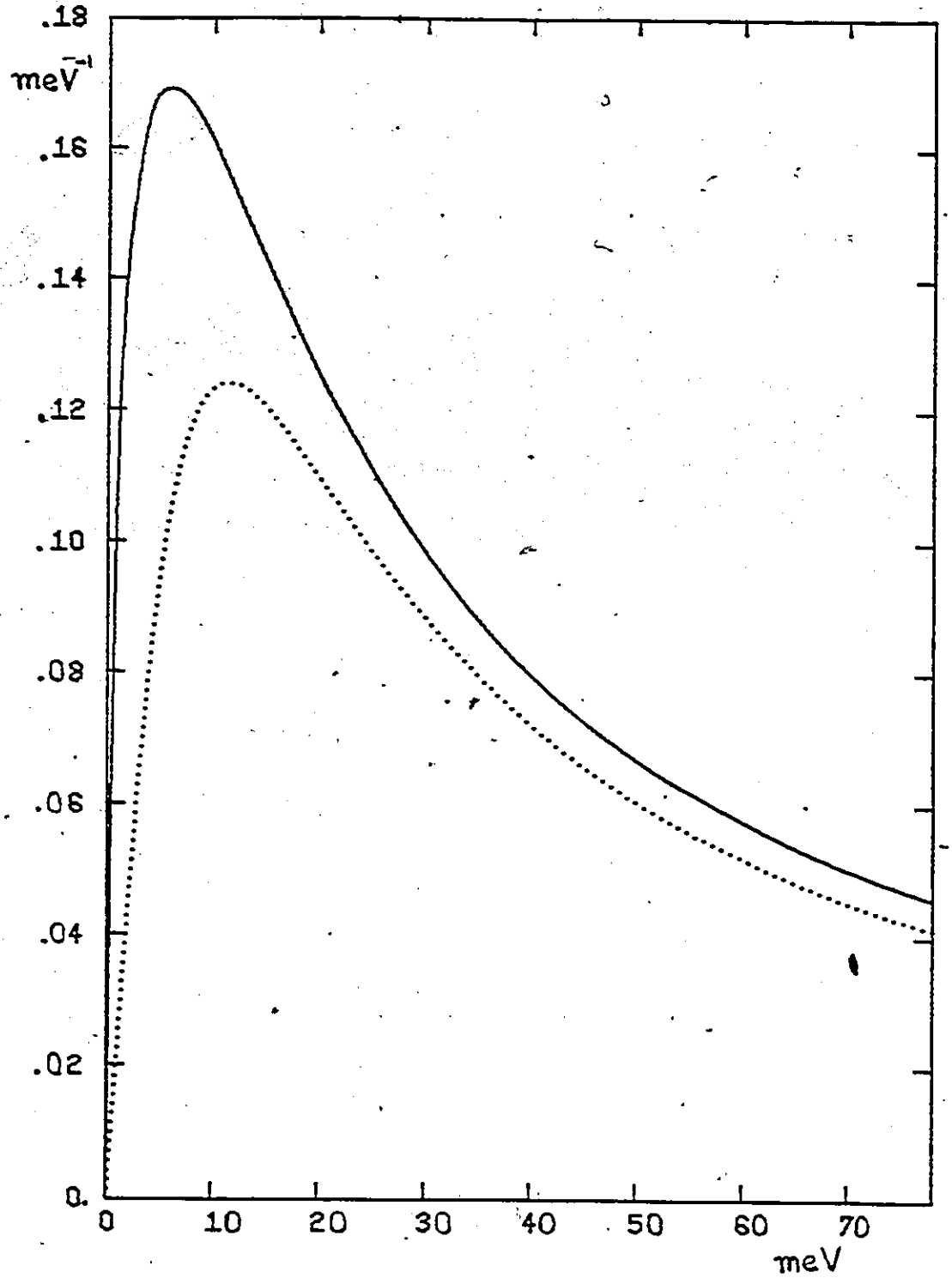
.18
meV⁻¹
.16
.14
.12
.10
.08
.06
.04
.02
0.
0
10
20
30
40
50
60
70
meV

the functional derivative $\delta\Delta_0/\delta\alpha^2(\Omega)F(\Omega)$ [27]

$$2\Omega^*(\Delta_0) \sim \Omega^*(T_c) \quad . \tag{4.7}$$

Second, for all four materials and frequencies considered

$$\frac{1}{\Delta_0}\frac{\delta\Delta_0}{\delta\alpha^2(\Omega)F(\Omega)} \geq \frac{1}{T_c}\frac{\delta T_c}{\delta\alpha^2(\Omega)F(\Omega)} \quad . \tag{4.8}$$

which implies (see formula (4.4))

$$\frac{\delta}{\delta\alpha^2(\Omega)F(\Omega)}\left(\frac{2\Delta_0}{k_B T_c}\right) \geq 0 \quad . \tag{4.9}$$

In Figure 5 we give the functional derivative $\delta(2\Delta_0/k_B T_c)/\delta\alpha^2(\Omega)F(\Omega)$ for all four materials. All of them are sharply peaked at $\Omega^*(\Delta_0)/3$ to within about 15% [27] where Δ_0 is corresponding value of the gap edge

$$\Omega^*\left(\frac{2\Delta_0}{k_B T_c}\right) = \frac{\Omega^*(\Delta_0)}{3} \quad . \tag{4.10}$$

In Figure 6, $T_c^{-1}\delta T_c/\delta\alpha^2(\Omega)F(\Omega)$ is plotted as a function of $\Omega/k_B T_c$ and in Figure 7 $\Delta_0^{-1}\delta\Delta_0/\delta\alpha^2(\Omega)F(\Omega)$ as a function of Ω/Δ_0 for all four materials. It can be seen that both these functional derivatives have a universal shape: both of them go to zero at $\Omega = 0$ and at large frequencies. $\delta T_c/\delta\alpha^2(\Omega)F(\Omega)$ peaks at a frequency $\Omega^*(T_c)$ which is within $\sim$ 15% of $8k_B T_c$ [27]

$$\Omega^*(T_c) \sim 8k_B T_c \tag{4.11}$$

FIG. 5

Functional derivative $\delta(2\Delta_0/k_BT_c)\delta\alpha^2(\Omega)F(\Omega)$ for Ta (-·-·-·-), Nb(·····), Pb(------) and Nb_3Sn (————).

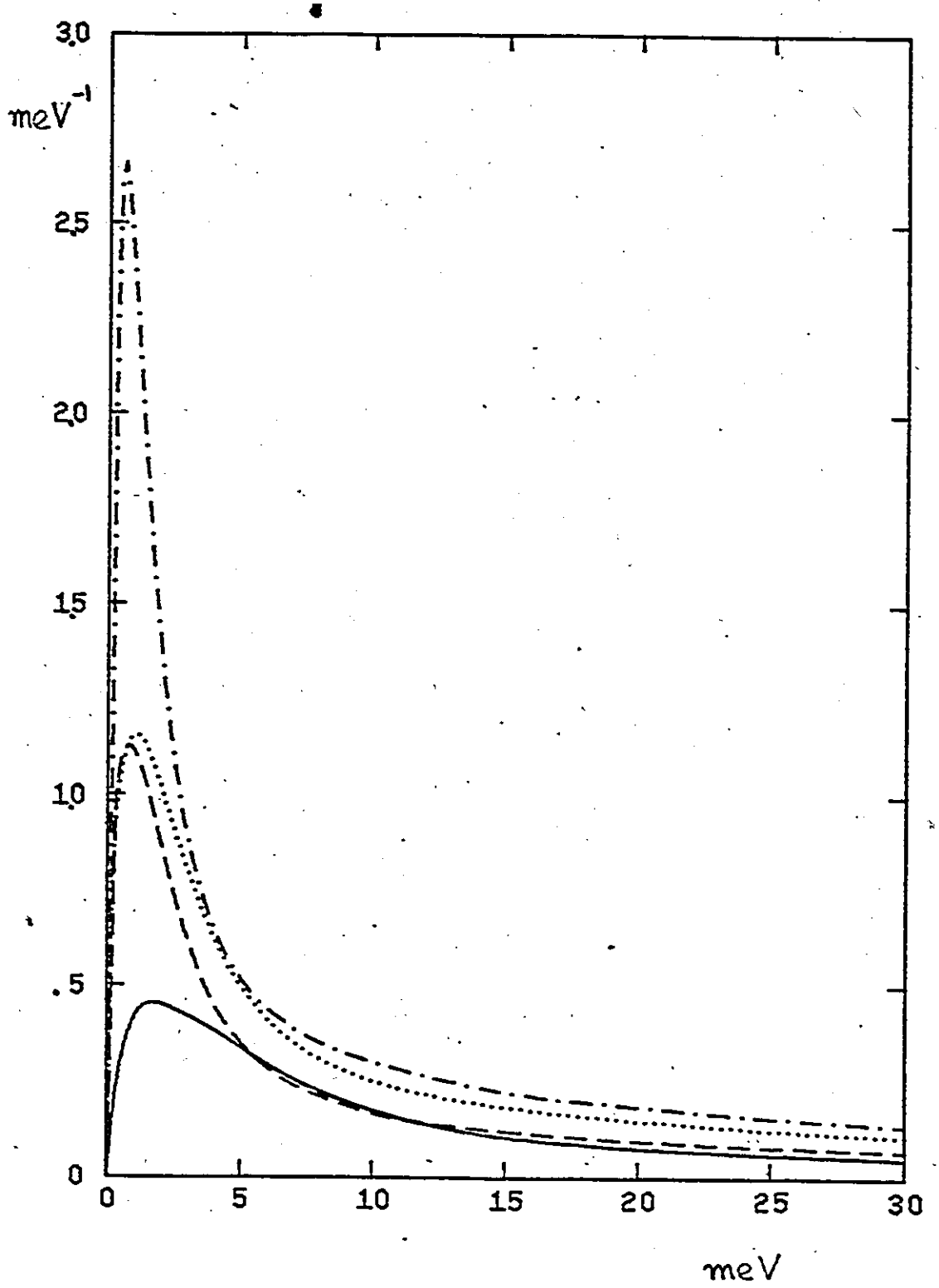
3.0
meV⁻¹
2.5
2.0
1.5
1.0
.5
0
0
5
10
15
20
25
30
meV

FIG. 6

$T_c^{-1}\delta T_c/\delta\alpha^2(\Omega)F(\Omega)$

For Ta (-·-·-·-·-·-), Nb(·····), Pb (------) and Nb_3Sn (———) as a function of Ω/k_BT_c.

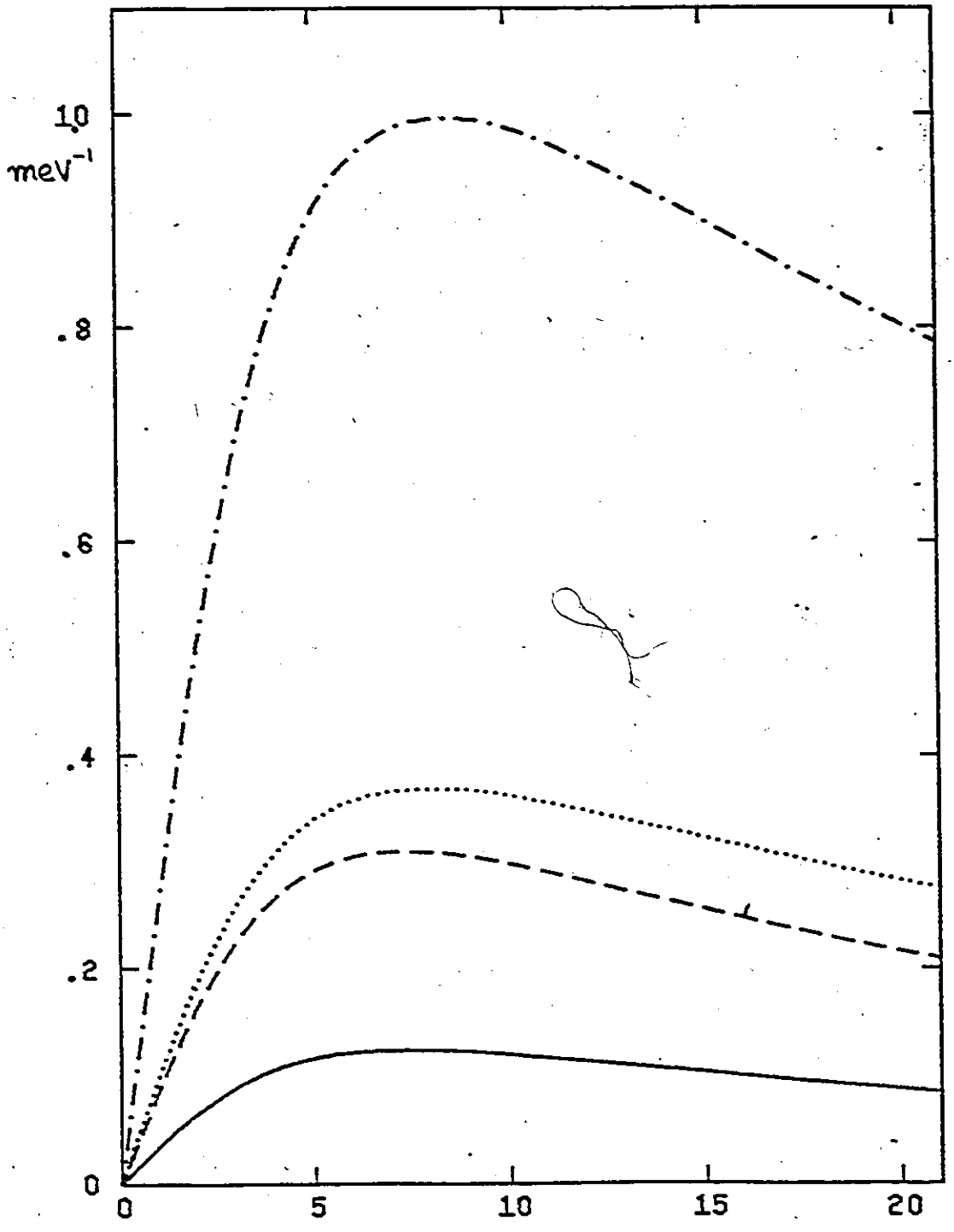
1.0
meV⁻¹
.8
.6
.4
.2
0
0
5
10
15
20

FIG. 7

$\Delta_0^{-1}\delta\Delta_0/\delta\alpha^2(\Omega)F(\Omega)$

Ta (----------), Nb (••••••), Pb (------) and Nb_3Sn (————) as a function of Ω/Δ_0.

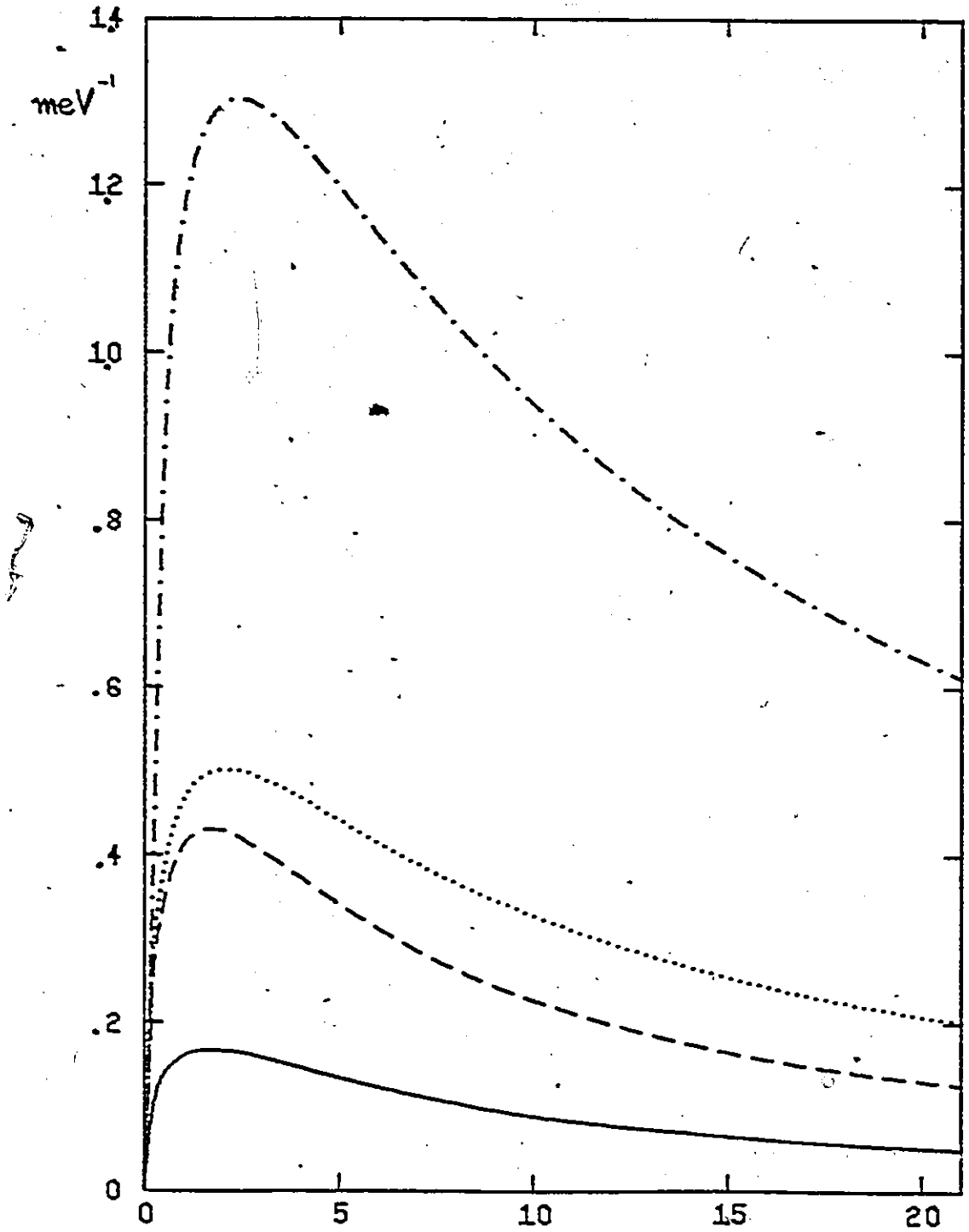
meV⁻¹
1.4
1.2
1.0
.8
.6
.4
.2
0
0
5
10
15
20

while $\delta\Delta_0/\delta\alpha^2(\Omega)F(\Omega)$ peaks at a frequency $\Omega^*(\Delta_0)$ which is within $\sim$ 20% at $2\Delta_0$ [27]

$$\Omega^*(\Delta_0) \sim 2\Delta_0 \quad . \tag{4.12}$$

One can sum up relations (4.7), (4.10) and (4.11) into a useful 'rule of thumb' [27]

$$6\Omega^*\left(\frac{2\Delta_0}{k_B T_c}\right) \sim 2\Omega^*(\Delta_0) \sim \Omega^*(T_c) \sim 8k_B T_c \tag{4.13}$$

Although we have considered only four different superconductors from various coupling regimes we can say that (4.13) can probably be applied to most, if not all 'dirty', that is isotropic, superconductors.

The universality of the shape of the functional derivatives $\delta T_c/\delta\alpha^2(\Omega)F(\Omega)$, $\delta\Delta_0/\delta\alpha^2(\Omega)F(\Omega)$ and $\delta(2\Delta_0/k_B T_c)/\delta\alpha^2(\Omega)F(\Omega)$ makes them useful in predicting qualitative changes in Δ_0, T_c and $2\Delta_0/k_B T_c$ due to small changes in electron-phonon spectral function $\alpha^2(\Omega)F(\Omega)$ with pressure, alloying, increasing disorder, etc.

Before we give an example of how these functional derivatives can be used in correlating qualitative changes in T_c, Δ_0 and $2\Delta_0/k_B T_c$ with changes in $\alpha^2(\Omega)F(\Omega)$ we give in Table 2 computed results for $T_c^{-1}\partial T_c/\partial\mu^*$, $\Delta_0^{-1}\partial\Delta_0/\partial\mu^*$ and $(2\Delta_0/k_B T_c)^{-1}\partial(2\Delta_0/k_B T_c)\partial\mu^*$ for Ta, Nb, Pb and Nb_3Sn. These derivatives can be used to correlate the changes in T_c, Δ_0 and $2\Delta_0/k_B T_c$ to small changes in Coulomb repulsion parameter μ^*.

Table 2

System	$T_c^{-1}\partial T_c/\partial\mu^*$	$\Delta_0^{-1}\partial\Delta_0/\partial\mu^*$	$(2\Delta_0/k_BT_c)^{-1}\partial(2\Delta_0 k_BT_c)/\partial\mu^*$
Ta	-6.2	-7.0	-0.8
Nb	-4.2	-4.8	-0.6
Pb	-2.1	-2.4	-0.3
Nb_3Sn	-2.1	-2.4	-0.3

As an example of correlating the qualitative changes in T_c, Δ_0 and the ratio $2\Delta_0/k_BT_c$ to the changes in $\alpha^2(\Omega)F(\Omega)$ and μ^* on the basis of various functional derivatives we take Nb[21] and alloy $Nb_{.75}Zr_{.25}$[25,28] (see Table 1). In Fig. 8 we plot the two spectra together with functional derivatives $\delta T_c/\delta\alpha^2(\Omega)F(\Omega)$ and $\delta\Delta_0/\delta\alpha^2(\Omega)F(\Omega)$. It can be seen that the alloying of Zr in Nb results in a considerable increase of the spectral weight below $\sim$ 10 meV for $Nb_{.75}Zr_{.25}$ with respect to Nb. This 'phonon softening' results in an increase of electron-phonon mass enhancement parameter λ from 1.01 for the Nb to 1.31 for $Nb_{.75}Zr_{.25}$ - a 30% increase. At the same time the total area A under $\alpha^2(\Omega)F(\Omega)$ is increased by only 2.5%. Therefore the overall change in the spectrum in going from Nb to $Nb_{.75}Zr_{.25}$ can be characterized to a good approximation by a shift of the spectral weight to the region

FIG. 8

$\alpha^2(\Omega)F(\Omega)$ for Nb (———), $\alpha^2(\Omega)F(\Omega)$ for $Nb_{.75}Zr_{.25}$ (·····), $\delta T_c/\delta\alpha^2(\Omega)F(\Omega)$ for Nb (-·-·-·-·-), $\delta\Delta_0/\delta\alpha^2(\Omega)F(\Omega)$ for Nb (------).

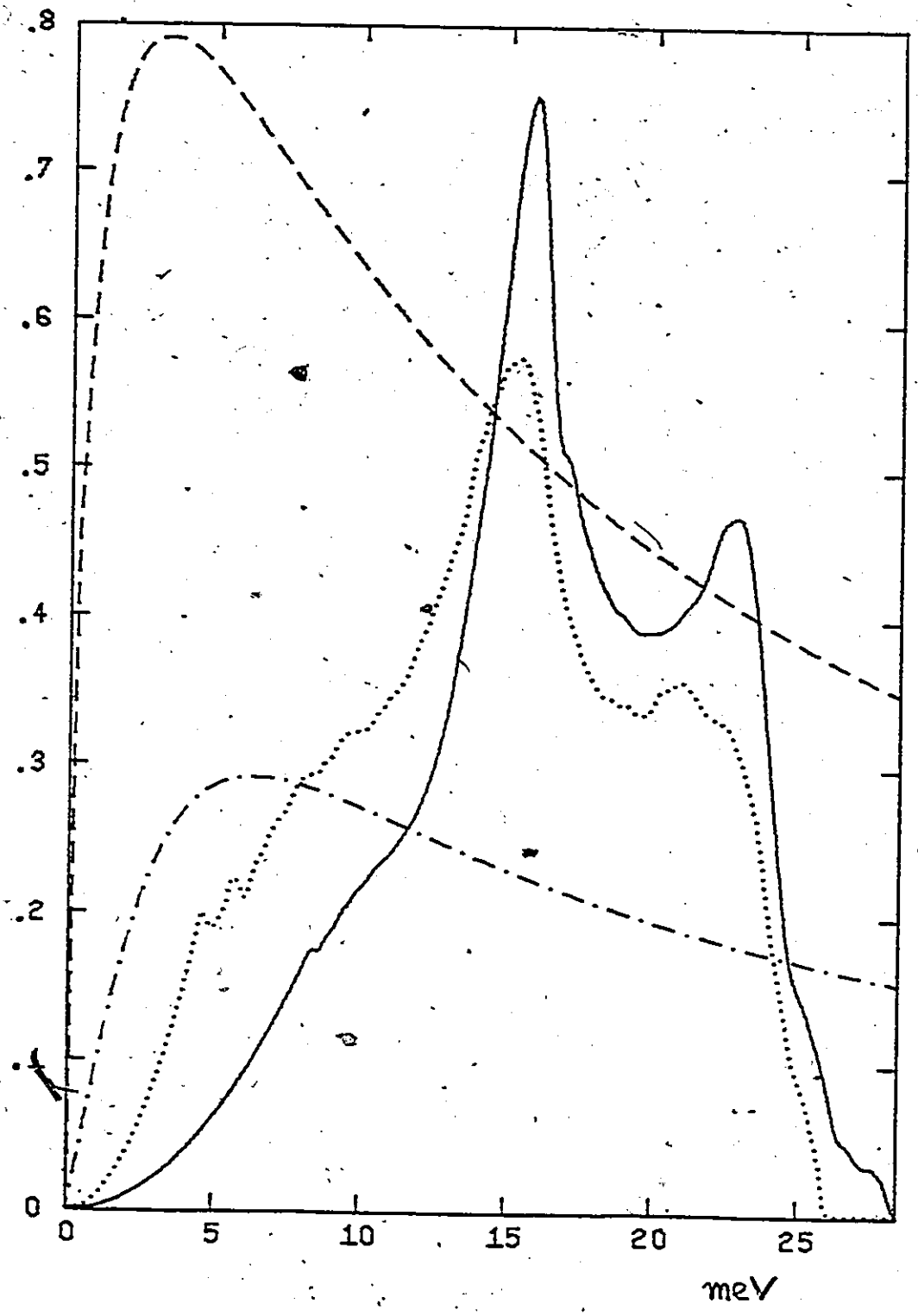
.8
.7
.6
.5
.4
.3
.2
.1
0
0
5
10
15
20
25
meV

below $\sim$ 10 meV. This region falls under the peaks of both functional derivatives of T_c and Δ_0 and therefore we can expect an increase in both of these quantities. However, since $\Delta_0^{-1}\delta\Delta_0/\delta\alpha^2(\Omega)F(\Omega)$ is larger than $T_c^{-1}\delta T_c/\delta\alpha^2(\Omega)F(\Omega)$ the gap edge Δ_0 should be increased more than the transition temperature T_c which would result in an increase in $2\Delta_0/k_BT_c$. We also note that the Coulomb repulsion parameter μ^* is decreased from 0.1854215 for Nb to 0.1807988 for $Nb_{.75}Zr_{.25}$ which should also result in an increase in T_c, Δ_0 and the ratio $2\Delta_0/k_BT_c$. However, this decrease is small, $\sim$ 0.004, and from the values of $T_c^{-1}\partial T_c/\partial\mu^*$, $\Delta_0^{-1}\partial\Delta_0/\partial\mu^*$ and $(2\Delta_0/k_Bt_c)^{-1}\partial(2\Delta_0/k_Bt_c)/\partial\mu^*$ given in Table 2 we estimate that the changes in T_c, Δ_0 and $2\Delta_0/k_BT_c$ due to a change in μ^* are $\Delta(T_c) \approx 0.15°K$, $\Delta(\Delta_0) \approx 0.03$ meV and $\Delta(2\Delta/k_BT_c) \approx 0.06$: these changes are small compared to the total changes $\Delta_{tot}(T_c) = 1.58°K$, $\Delta_{tot}(\Delta_0) = 0.39$ meV and $\Delta_{tot}(2\Delta_0/k_BT_c) = 0.27$. Therefore the largest part of the increase in T_c, Δ and $2\Delta_0/k_BT_c$ in going from Nb to $Nb_{.64}Zr_{.25}$ is due to the shift of electron-phonon spectral weight to a more favorable region of frequencies.

Mitrović and Carbotte[29] have also successfully explained the trends of Δ_0, T_c and $2\Delta_0/k_BT_c$ in the Pb-Bi alloy series on the basis of various calculated functional derivatives. Further applications of functional derivatives to the quenched Hg-films and Pb-films as well as to a critical dis-

cussion of an often used simple formula for the ratio $2\Delta_0/k_BT_c$ are given by Mitrović, Leavens and Carbotte[27].

SUMMARY

In Chapter III we have applied the method of N-point Padé approximants to calculate the ratio $2\Delta_0/k_BT_c$ from Eliashberg theory, for over thirty superconductors. To do this we have first solved the linearized Eliashberg equations on the imaginary axis with the Coulomb repulsion parameter μ^* chosen to reproduce the experimental critical temperature T_c and then used the same μ^* value to solve the Eliasberg equations on the imaginary axis at some low temperature T_c. Then we have applied the method of N-point Padé approximant to analytically continue the imaginary axis solution to the real frequency axis and so determine the gap edge Δ_0 from the relation Re $\Delta(\omega=\Delta_0,T) = \Delta_0$. The fact that this method worked perfectly in the case of Pb and Hg where it is known that strong coupling theory works well and where the tunneling experiments can be performed without any difficulty, indicate that we can use it in predicting the values $2\Delta_0/k_BT_c$ on the basis of standard Eliashberg theory for other superconductors for which we had data on $\alpha^2(\Omega)F(\Omega)$. In the case of Al we have shown that Eliashberg theory gives the correct weak coupling limit (that is the BCS result). For the great majority of the superconductors considered, the calculated values of Δ_0, that is $2\Delta_0/k_BT_c$ were in good agreement with

experimental results. In this way it was shown that standard Eliashberg theory can account for the observed values of the ratio $2\Delta_0/k_BT_c$ in almost all cases we have considered. In a few cases, of poor agreement, where the errors were of the order 8% - 14%, the discrepancies can be related to the difficulties with forming good tunneling junctions as is known to be the case for Nb, or perhaps to not sufficiently accurate measurements of Δ_0 and/or T_c. Of course, it may well be that for certain materials the standard Eliashberg formulation of the theory should be modified to better account for the particular properties of these materials. This is the objective of some present studies in the theory of superconductivity.

In Chapter IV we have presented accurate numerical calculations of functional derivatives $\delta\Delta_0/\delta\alpha^2(\omega)F(\omega)$ and $\delta(2\Delta_0/k_BT_c)/\delta\alpha^2(\Omega)F(\Omega)$ for Ta, Nb, Pb and Nb_3Sn. In our numerical work we have used the method of N-point Padé approximants to calculate the changes in the gap edge due to small variations in electron-phonon spectral function $\alpha^2(\Omega)F(\Omega)$. In calculating the functional derivative $\delta(2\Delta_0/k_BT_c)/\delta\alpha^2(\Omega)F(\Omega) = (2\Delta_0/k_BT_c)(\Delta_0^{-1}\delta\Delta_0/\delta\alpha^2(\Omega)F(\Omega) - T_c^{-1}\delta T_c/\delta\alpha^2(\Omega)F(\Omega))$; the $T_c^{-1}\delta T_c/\delta\alpha^2(\Omega)F(\Omega)$ term was calculated from the imaginary frequency axis program written by Dr. J. M. Daams[13]. The calculated functional derivatives have a universal form[27]: they increase from zero at $\Omega = 0$,

peak at some frequency Ω^* and then decrease towards zero at large frequencies. The relation between the frequencies where various functional derivatives peak can be summarized by the relation[27]: $6\Omega^*(2\Delta_0/k_BT_c \sim 2\Omega^*(\Delta_0) \sim \Omega^*(T_c) \sim 8k_BT_c$. Although we have considered only four superconducting materials of various coupling strengths our conclusions probably can be applied to all superconducting materials in the isotropic limit. The universal shape of these functional derivatives makes them useful in correlating qualitative changes in T_c, Δ_0 and $2\Delta_0/k_BT_c$ to small changes in electron-phonon spectral function. In particular the above simple relation between various peak frequencies can be used for rough estimates. We have shown how one can successfully use various calculated functional derivatives to understand the difference in the superconducting properties of $Nb_{.75}Zr_{.25}$ and Nb.

REFERENCES

1) J. R. Schrieffer, Theory of Superconductivity, Benjamin, New York, 1964).

2) D. J. Scalapino, J. R. Schrieffer, and J. W. Wilkins, Strong-coupling superconductivity. I, Phys. Rev. 148, 263 (1966).

3) D. J. Scalapino, The Electron-phonon interaction and strong-coupling superconductors, in Superconductivity, ed. by R. D. Parks, (Marcel Dekker, New York, 1969).

4) V. Ambegaokar, Strong coupling superconductors, in Probléme À N Corps, Many-Body Physics, édité par C. De Witt, R. Balian, (Gordon and Breach, New York, 1968).

5) J. C. Swihart, Phys. Rev. 131, 73 (1963).

6) Y. Wada, Rev. Mod. Phys. 36, 253 (1964).

7) J. P. Carbotte, Strong Coupling Superconductivity, Lecture notes from Escuela Latino Americana de Fisica (Universidad Nacional Autonoma de México, México, D.F. 1974).

8) P. B. Allen, Phys. Rev. B6, 2577 (1972).

9) W. H. Butler, H. G. Smith and N. Wakabayashi, Phys. Rev. Lett. 39, 1004 (1977).

10) J. M. Rowell, W. L. McMillan, and R. C. Dynes, A Tabulation of the Electron-phonon Interaction in Metals and Alloys. Part I, private communication.

11) C. R. Leavens, private communication.

12) G. Bergmann and D. Reiner, Z. Physik, 263, 59 (1973); D. Reiner and G. Bergmann, J. Low Temp. Phys. 14, 501 (1974).

13) J. M. Daams, Ph.D. Thesis, McMaster University, Hamilton, Ontario 1977.

14) H. J. Vidberg and J. W. Serene, J. Low Temp. Phys. 29, 179 (1977).

15) G. A. Bauer Jr., Essentials of Padé Approximants, (Academic Press, New York, 1975).

16) L. Y. Shen, Phys. Rev. Lett. 29, 1082 (1972).

17) D. F. Moore, R. B. Zubeck, J. M. Rowell and M. R. Beasley, Phys. Rev. B20, 2721 (1979).

18) D. F. Moore, M. R. Beasley and J. M. Rowell, Journal de Physique, Colloque C6, Supplement au No. 8, Tome 39 (1978).

19) J. M. Rowell, private communication; also B. Robinson and J. M. Rowell in Transition Metals 1977, Inst. Phys. Conf. Ser. No. 39 (1978).

20) G. B. Arnold, J. Zasadzinski, and E. L. Wolf, Phys. Lett. 69A, 136 (1978).

21) G. B. Arnold and E. L. Wolf, private communication.

22) W. H. Butler, private communication.

23) J. Bostock, K. H. Lo, W. N. Cheung, V. Diadiuk and M. L. A. MacVicar in Rochester Conference on Superconductivity in d- and f-band Metals, 20, 1976, ed. by D. H. Douglass (Plenum Press, 1976).

24) H. Rietschel and H. Winter, Phys. Rev. Lett. 43, 1256 (1979).

25) E. L. Wolf, private communication; E. L. Wolf and R. J. Noer, Sol. State Comm. 30, 391 (1979).

26) H. K. Leung, J. P. Carbotte, D. W. Taylor and C. R. Leavens, J. Low Temp. Phys. 24, 2534 (1976).

27) B. Mitrović, C. R. Leavens and J. P. Carbotte, to be published.

28) B. Mitrović and J. P. Carbotte, to be published.

29) B. Mitrović and J. P. Carbotte, to be published.

30) R. R. Chen, J. D. Chen, J. D. Leslie and H.J.T. Smith, Phys. Rev. L355. 22 (1969).

31) T. T. Chen, Ph.D. Thesis, The University of Waterloo (1969).